

Advancing Nuclear Astrophysics Using Next-Generation Facilities and Devices

C. Langer^a, N. Klapper^a, C. Köppchen^a, S. Dababneh^b and R. Reifarth^a

^a Goethe University Frankfurt, Frankfurt, Germany.

^b Department of Physics, Faculty of Science, Al-Balqa Applied University, Salt, Jordan.

Received on: 23/8/2017;

Accepted on: 18/12/2017

Abstract: Where are all the heavy elements formed? How are they formed? What is the role played by stars and stellar explosions?

Nuclear astrophysics aims at answering these fundamental scientific questions by linking nuclear physics with astrophysical modelling and observations. Large progress has been achieved in past decades. However, new nuclear physics facilities and devices are urgently required to advance research into regions of the nuclear chart so far not reachable. This will enable unprecedented studies of nuclear reactions in the laboratories, which are key for heavy element synthesis and the fate of a star. Some highlights of upgrade-in-process will be described.

Experimental effort needs to be guided by astrophysical modelling to find significant uncertainties and pinpoint important measurements to be carried out. For two astrophysical scenarios, sensitivity studies using detailed nuclear network calculations will be presented. These calculations involve charge-particle induced reactions like (p,γ) or (α,γ) during the rapid proton capture process (rp process). On the other hand, core-collapse supernovae can be studied using rare presolar type C SiC grains. Observed peculiar abundance distributions in these grains can be explained with the conditions during the nucleosynthesis. We therefore study the light mass Si-S region by variations of (n,γ) reaction rates. Also, the influence of different neutron pulses and the effect on the final abundances of the production of the important radioisotope ^{32}Si are examined.

Both investigations stress the need for enhanced experimental approaches to measure reaction rates to better constrain the astrophysical sites.

Keywords: Nuclear astrophysics, Presolar grains, Nuclear physics, Facilities, Network calculations.

Introduction

Nuclear reactions play a dominant role for the energy generation of stars. Fusion reactions during the hydrostatic evolutionary phases of a star lead to a partial creation of heavy chemical elements up to iron-like elements [1,2].

Elements beyond iron must be produced in other processes. In a ground-breaking publication [3], the authors describe several processes involving particle captures on existing seed nuclei for creating the heaviest observed

elements. Up to now, our understanding is still based on the same idea: all heavy elements must be created in stars and stellar explosions. However, the fine details of the different production mechanisms have been shaped and changed over the past 50 years and it seems that the grand picture is settled, see e.g. [4–8].

To create heavy elements, several distinct processes act in our surrounding universe, like the slow and rapid neutron capture processes (s-

and r-process) at different stellar sites. Input from nuclear physics, like cross-sections, reaction rates, masses, binding energies, half-lives and others, are key for understanding the details of these production mechanisms. For stable or close-to-stable isotopes, many of the required properties have been determined and can be used in astrophysical modelling and galactical chemical evolution calculations [9].

However, several heavy element production processes involve highly radioactive isotopes far off the valley of stability. To study them experimentally, special radioactive science facilities are required for production of short-lived isotopes as a beam. It is then possible to examine relevant astrophysical reactions; however, many measurements still need to be carried out and are urgently required for advancing astrophysical calculation. Currently, the limitation of existing facilities is reached and further progress is hampered. Therefore, major upgrades are foreseen at several facilities all over the world.

To guide upcoming experiments towards the important, so far inaccessible, reactions, detailed astrophysical and nuclear calculations are required. Nuclear network calculations can be used to better understand abundance flows and uncertainties in input parameters, like reaction rates and masses, and disentangle them from thermodynamic effects imposed by the specific astrophysical environment.

The next section of this article will shortly motivate the need for new and upgraded facilities and devices. All the experimental effort should be guided by comprehensive astrophysical calculations. Therefore, detailed network calculations for the rapid proton capture process on neutron stars are shown. Also, the influence of uncertain reaction rates on a recently discovered peculiarity in the expected abundance distribution extracted from presolar SiC grains will be discussed and first preliminary results will be shown. This potentially leads to a better understanding of core-collapse supernovae and their contribution to the formation of SiC grains.

Future Facilities and Devices

Major upgrades are foreseen at current facilities. The focus is on producing more exotic isotopes at higher intensities and better quality. This will finally enable experimental studies

involving the very short-lived isotopes relevant for stellar modelling, which, in turn, will also lead to a highly-increased understanding of the details of how a nucleus arranges and what the underlying forces are. This is complemented by very active research in nuclear theory and a constant increase in computer power, which in turn enables calculations from first principles even for heavier isotopes, see e.g. [10].

A good overview of ongoing upgrades and future facilities can be found e.g. here [11–23].

Besides establishing upgraded beam facilities, major effort is also put into the development of new equipment and devices relevant for nuclear astrophysics. Next-generation setups, like e.g. the R^3B setup [24,25] and CRYRING at FAIR [26], as well as SECAR [27] and the high-rigidity spectrometer at FRIB [28], are extremely important tools for studying processes significant in nuclear astrophysics. They will allow for a multitude of different reaction studies with which key properties, like reaction rates and masses, can be extracted, even with lowest intensity beams.

Also, new devices will unfold their full potential once the desired upgrades are successfully completed. As an example, it has been shown recently that γ -ray detection devices, like GRETA [29,30] (similar to AGATA [31]) are very powerful instruments for studies related to nuclear astrophysics [32–36]. Using them in conjunction with a magnetic spectrometer and a radioactive beam facility, nuclear structure properties can be extracted, that are in turn sensitively entering the reaction rates.

Network Calculations

Performing nuclear reaction experiments is typically a very tedious task and employs a lot of effort and manpower. Therefore, ideally, (future) experiments performed for nuclear astrophysics should be guided by detailed astrophysical calculations estimating the impact of a certain reaction in a specific astrophysical environment.

In this sense, nuclear reaction network calculations represent a powerful tool. Here, the interaction of several isotopes connected through corresponding reactions, like (p,γ) or (n,γ) , as well as weak decays, like β -decays, can be studied in terms of energy generation, abundance formation and other interesting properties. This typically includes solving coupled differential

equations and requires special tools to handle the (huge) amount of processing time. To study the effect induced by nuclear physics, like uncertainties in the reaction rate, these network calculations can be performed using different input parameters. This can then be, in turn, compared to base runs, in which no variations are included. Eventually, the effect of single or multiple uncertainties in a specific network calculation can be assessed.

In the following sections, two examples of preliminary detailed network calculations will be presented related to different astrophysical scenarios. Both estimate the impact of uncertain reaction rates on observables, like X-ray burst light curves and abundance distributions, on presolar SiC grains.

a. Type I X-ray Bursts

Type I X-ray bursts are thermonuclear explosions ignited in the outer envelope of an accreting neutron star. Because of the constantly rising temperatures and densities during the accretion process, eventually, a thermonuclear runaway might be triggered.

This, in turn, leads to high temperatures up to 2 GK and typical densities of 10^6 g/ccm. Depending on the composition of the accreted material, which is typically hydrogen- and helium-rich, fast proton- and alpha-capture reactions are driving the initial light material towards heavier elements, and up to $A = 100$ can be created in this so-called rapid proton capture process (rp process); i.e., adding more than 50 protons to the initial H/He material [37, 38]. In total, this takes only a few seconds and is typically repeated while the neutron star accretes again material from the companion star.

These explosions can be observed using space-based telescopes as an outburst of the X-ray luminosity with a specific shape of a fast rise and a slow exponential-like decay.

It is still an open question whether the produced ashes of the explosion enrich the surrounding interstellar medium through mass loss or other mechanisms. It still seems that type I X-ray bursts do not contribute to the observed solar abundance distribution.

Nonetheless, observation of type I X-ray bursts offers unique and exciting insights into nuclear physics under extreme conditions on a neutron star, as well as the behavior of dense

neutron matter; as such, this type of X-ray bursts is deemed to represent a very rich stellar nuclear laboratory, e.g. [39,40].

Extracting astrophysical information from X-ray burst light curves, like accretion rate, composition, millisecond oscillations and others, requires a detailed understanding of the underlying nuclear physics and the reactions among different nuclei. Therefore, the existing uncertainties in key nuclear reactions must be eliminated or at least significantly constrained. In recent sensitivity studies [41–44], the influence of these nuclear physics uncertainties on the light curves and abundance distributions has been studied and evaluated.

Sensitivity Study

In this study, we focus on the major rp process waiting point ^{56}Ni . Because of its peculiar properties, it serves as a dominant bottleneck in the rp process. The ^{56}Ni isotope decays almost exclusively *via* electron capture (EC) decay to ^{56}Co , since the β^+ -decay is blocked. This, however, takes more than 10^4 seconds and is as such not possible in typical X-ray burst scenarios. The breakout reaction $^{56}\text{Ni}(p,\gamma)^{57}\text{Cu}$, on the other hand, has a relatively low Q value of only 690 keV, which leads to a fast buildup of flow equilibrium between the forward (p, γ) and the reverse (γ ,p) reaction under hot conditions (similar to the r process waiting point picture). Heavier, charged particle-induced reactions are typically hampered by the already high Coulomb barrier.

In a recent study, the influence of the breakout reaction on ^{57}Cu ; i.e., $^{57}\text{Cu}(p,\gamma)^{58}\text{Zn}$, was studied to understand the reaction flow $^{56}\text{Ni}(p,\gamma)^{57}\text{Cu}(p,\gamma)^{58}\text{Zn}$ [32]. A second study determined a new $^{55}\text{Ni}(p,\gamma)^{56}\text{Cu}$ rate, which could lead to a significant bypass of ^{56}Ni , when enough material is being processed towards ^{57}Zn [34]. The $^{56}\text{Ni}(p,\gamma)^{57}\text{Cu}$ rate was already experimentally constrained by Rehm et al. [45].

Here, we study in detail the flow behavior around ^{56}Ni including several isotopes in the direct vicinity, see FIG. 1(a). This leads to a much better understanding of important and still uncertain reactions, which urgently need to be studied experimentally.

For solving the network equations, the code “xnet” has been used [46] with its input from the current JINA reaclib library [47]. The network is

then solved under fixed temperature and density conditions in the range of typical X-ray bursts. In FIG. 1(b), the β^+ decay ratio of ^{57}Zn for the $N = 27$ isotonic chain is calculated according to:

$$\beta^+ (^{57}\text{Zn}) = \frac{\beta_{57\text{Zn}}}{\beta_{56\text{Cu}} + \beta_{57\text{Zn}}},$$

with β_x being the partial integrated β^+ flows.

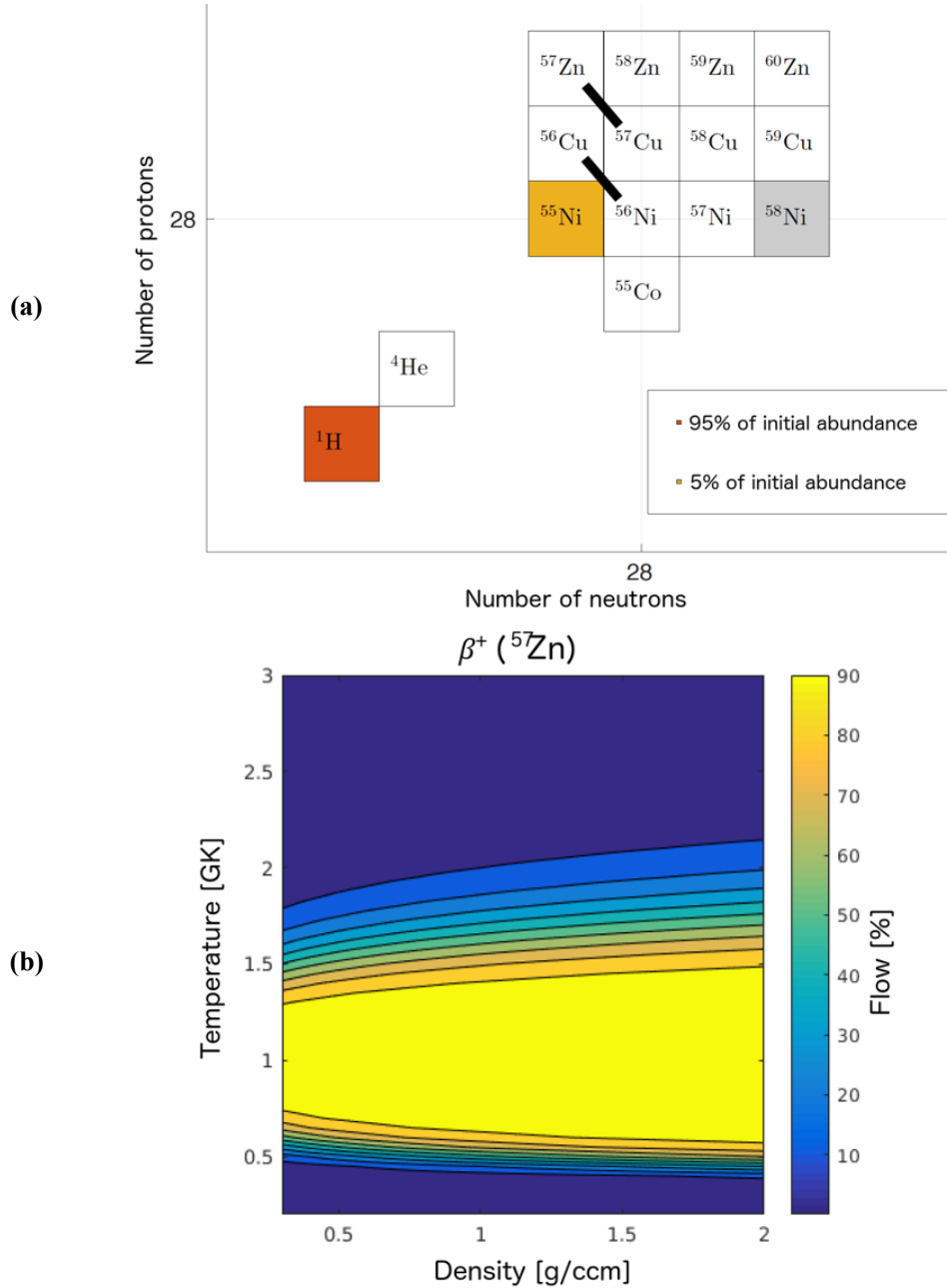


FIG. 1. (a) Small part of the rp process reaction network studied here. It includes nuclides near the major waiting point ^{56}Ni to the next waiting point ^{60}Zn . Within this small network, reaction rates, initial abundances, temperatures and densities can be varied and the effect on the flow can be studied. Two example β^+ flows are shown. (b) A typical result extracting the amount of leakage out of a certain isotonic chain to the next chain *via* β^+ decay. In this case, the decay out of the $N = 27$ isotonic chain (^{56}Cu , ^{57}Zn) into $N = 28$ is studied. Shown is the amount of flow given by β^+ decay of ^{57}Zn normalized to the total β^+ decay flow out of $N = 27$ in this network. This ratio is calculated for different temperature and density conditions, which are kept constant.

It is obvious that in a certain temperature and density region, more than 50% of the β -decay flow out of $N = 27$ is determined by the decay of ^{57}Zn . This can also be clearly seen in the flow pattern in FIG. 2. At a temperature of $T = 1$ GK

at $\rho = 10^6$ g/ccm, almost all the flow proceeds through ^{57}Zn , whereas, according to FIG. 1 and FIG. 2, at 2 GK, less than a few percent proceeds through the β -decay of ^{57}Zn .

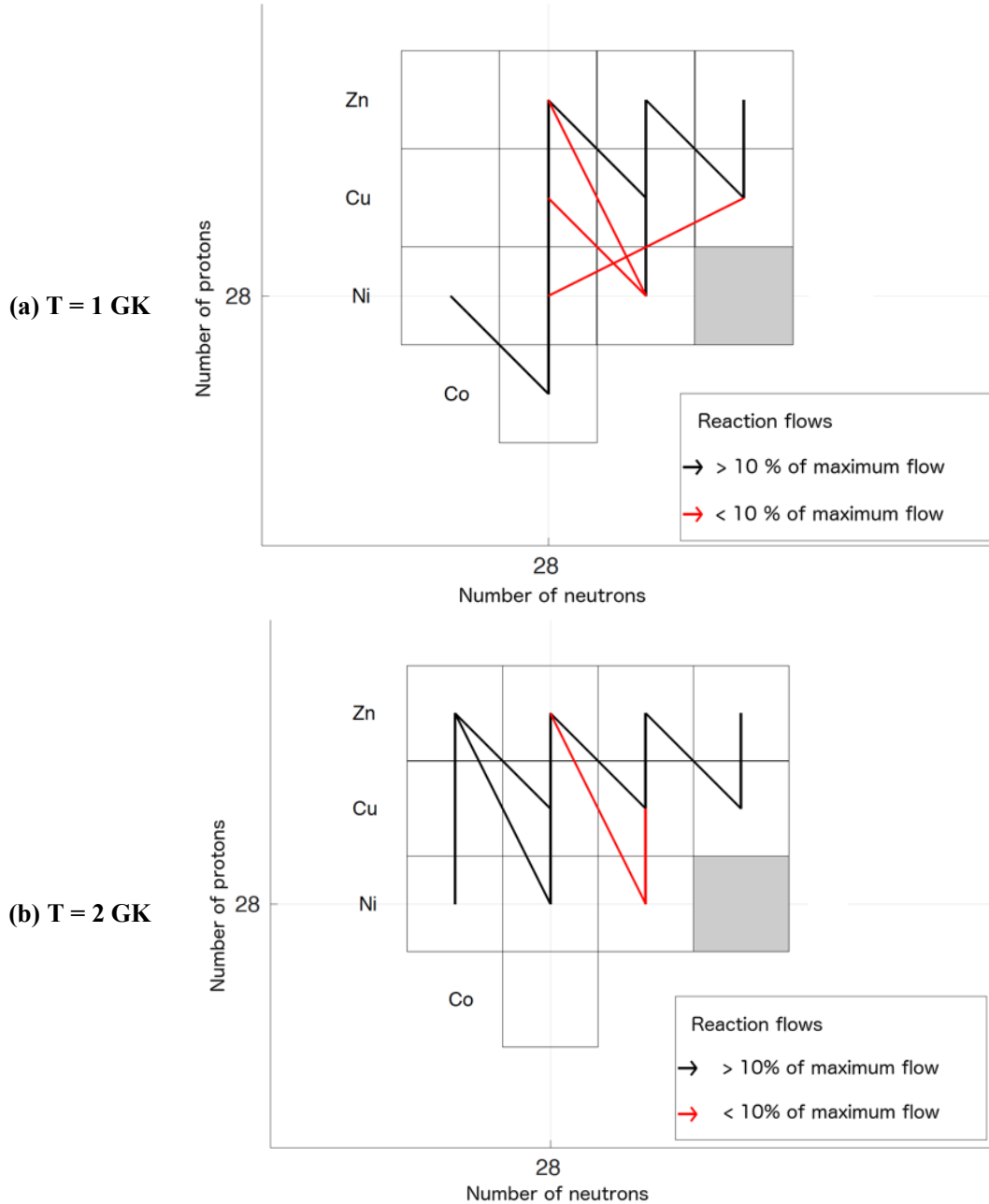


FIG. 2. Detailed calculations to examine the flow of the rp process under different temperatures in the ^{56}Ni region. For both figures, the density is set to 10^6 g/ccm. Black lines show dominant flow (i.e., more than 10% of the total flow) compared to the red lines, which show minor flows (less than 10% of the total flow). Clearly, in (b) at 2 GK, the $^{56}\text{Ni}(\alpha, p)$ and its reverse reaction $^{59}\text{Cu}(p, \alpha)$ start to contribute to the reaction flow. Also, the β -delayed proton emission decay is clearly visible under both temperature conditions.

As can also be seen in FIG. 2(b), the $^{59}\text{Cu}(p, \alpha)^{56}\text{Ni}$ starts to play a role when increasing the temperature. In fact, this reaction

feeds back into ^{56}Ni , whereas the reverse reaction $^{56}\text{Ni}(\alpha, p)^{59}\text{Cu}$ is much slower, thus contributing only little to the overall flow, see

FIG. 3(a). This leads to a sensitive temperature-dependence of the flow beyond ^{56}Ni , eventually trapping all material in ^{56}Ni at temperatures exceeding 2 GK. As this is barely in accordance

with astronomical observations, temperatures above 2 GK are very unlikely for standard type I X-ray bursts. This again shows the power of these detailed sensitivity studies.

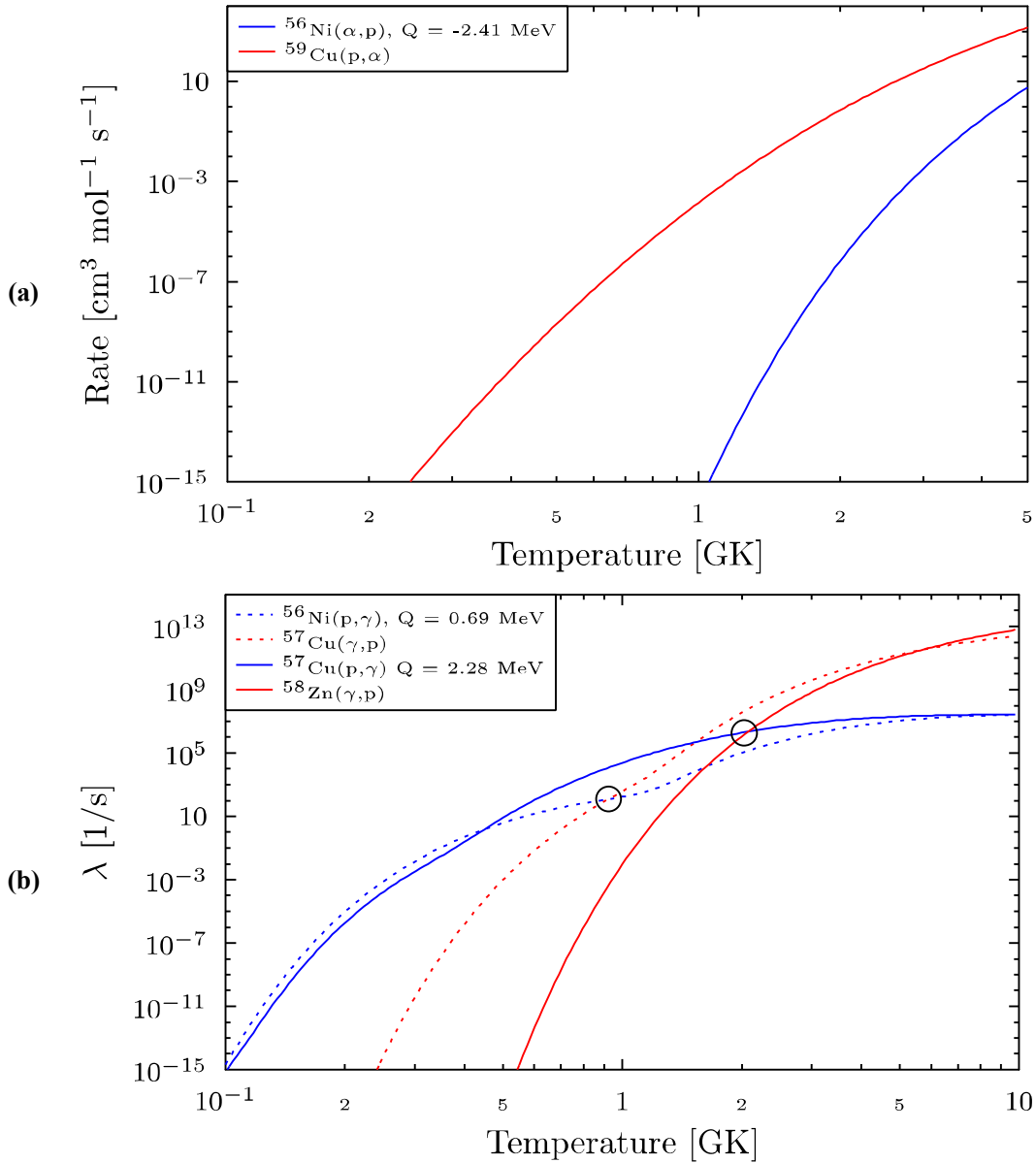


FIG. 3. (a) The $^{56}\text{Ni}(\alpha, p)$ rate with its reverse rate. As can be seen, the red line; i.e., the (p, α) reaction, is much faster than the forward (α, p) reaction (blue line) at typical X-ray burst temperatures. (b) Two different fast (p, γ) reactions (with a density of 10^6 g/cm^3 and a hydrogen mass fraction of 0.7) with the corresponding photodissociation rates. At a certain temperature T_{equal} , the photodissociation (γ, p) is getting faster than the forward reaction. This is a function of the Q value of the reaction (see black circles for different Q values).

FIG. 3(b) demonstrates thereby an important effect caused by the calculation of the reverse reaction using the detailed balance theorem in the case of a photodissociation reaction involved:

$$\frac{\lambda_{\gamma}}{N_A \langle \sigma v \rangle_{aA \rightarrow \gamma B}} \propto (k_B T)^{3/2} e^{-\frac{Q_{aA \rightarrow \gamma B}}{k_B T}},$$

with N_A being the Avogadro constant, $\langle \sigma v \rangle$ being the reaction rate with Maxwellian velocity

distribution, k_B the Boltzmann constant, T the temperature and Q the specific reaction Q value.

At a certain temperature T_{equal} , the reverse and the forward reaction are equally fast, as

shown with circles in FIG. 3(b). This temperature T_{equal} depends on the reaction Q value under same stellar environments.

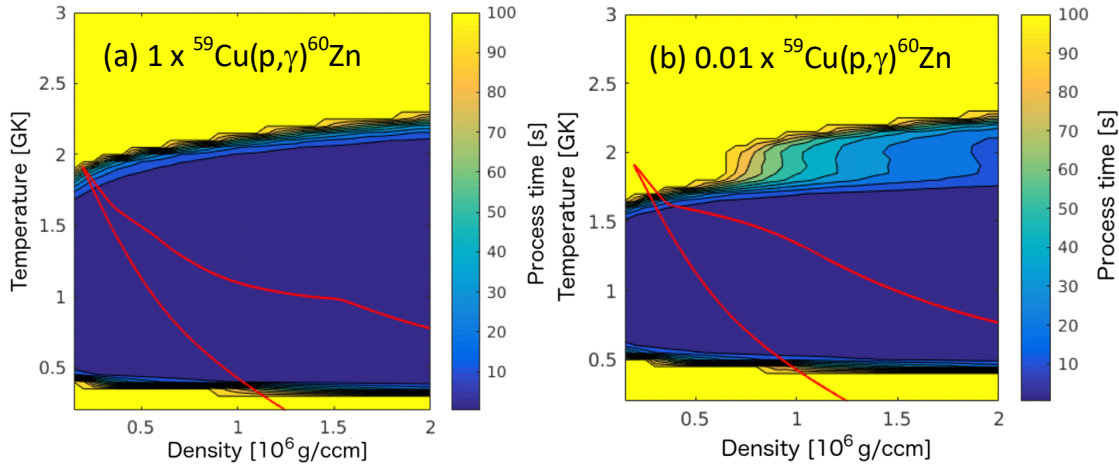


FIG. 4. Sensitivity study when varying one single reaction rate in (b). In this case, the important $^{59}\text{Cu}(p,\gamma)^{60}\text{Zn}$ reaction rate is varied by a factor of 0.01 from (a) to (b). To define a reasonable figure-of-merit, the processing time; i.e., how long it takes to move a certain fraction of the initial abundance through ^{56}Ni to ^{60}Zn , is studied here. This processing time is directly reflected in the main observable; the X-ray luminosity.

Recent sensitivity studies on X-ray bursts are based on a certain thermodynamic profile of the system, calculated in hydrodynamical stellar evolution codes, like KEPLER or others [41–43]. In [41], these self-consistent multizone models are used to calibrate a single zone model, which sensitively depends on the initial thermodynamic conditions (temperature and pressure). As such, the results are biased by the choice of a special code and a unique burst behaviour.

The approach taken here is to keep the sensitivity study as independent as possible from an underlying stellar model. Eventually, different thermodynamic trajectories can be inserted into the results presented here and the effect on different variables can be at least estimated.

An example is shown in FIG. 4. It shows the processing time depending on the density and temperature of the system. The processing time is defined as the time it takes to build up half of the initial abundance at the next waiting point, which is in this case ^{60}Zn . This processing time is directly influencing the observable light curve.

The $^{59}\text{Cu}(p,\gamma)$ rate is varied by a factor of 0.01 in FIG. 4(b) and then compared to the base run with no variation shown in FIG. 4(a). Different thermodynamic trajectories can also be seen. Especially at low density and high temperature, a

significant difference between the two cases can be seen. This difference in the processing time is reflected in a significant discrepancy between the predicted light curves with and without variation of $^{59}\text{Cu}(p,\gamma)$, as shown in [41]. The study performed here has a clear advantage; once a thermodynamic trajectory is known, (a) the effects on observables can be estimated by overlaying the trajectory with the results shown in FIG. 4, and (b), a detailed explanation of the effect can be provided (e.g. when and at which densities and temperatures this effect would be observed too, or could be neglected).

For the future, this approach needs to be expanded to study the entire rp process and cover more density and temperature ranges. Also, a Monte Carlo variation of single reaction rates can be used to complement the evaluation shown here. This would give more and clearer hints towards important reactions and will anticipate different reaction studies. More preliminary results and details about the technique can be found in [48].

b. The ^{32}Si Puzzle

Core-collapse supernovae mark the end of the evolution of massive stars and are extremely powerful explosions. They provide conditions, in which heavy element synthesis could take place. Still, our understanding of type II (core-collapse)

supernovae is very limited, although decades of research have been invested, see e.g. [49–51].

The grand picture is settled; however, details on the exact explosion mechanism, the formation of a neutron star from the proto-neutron star, the energy transport and other mechanisms, are still under active debate. Connected to these processes is the question of element synthesis, which severely depends on the formation of a neutron- or proton-rich environment inside the star shortly after the explosion was triggered [52]. However, information from inside the explosion region is very scarce, but provides important imprints of the actual conditions.

Tiny presolar grains offer an extremely interesting, unique and promising way to gain insight into the abundance distribution in certain regions of the star shortly after the explosion was triggered, see e.g. [53–57]. Once the temperatures are sufficiently low, these grains are condensed quite some time after the material was created inside the star. These distinct conditions, under which the material was produced, can be extracted by tracing certain isotope abundances (like e.g. ^{44}Ti) and then be connected to a particular stellar site.

A large amount of collected presolar grains is made of the SiC mineral. By far, most of the SiC grains are produced in AGB stars with different metallicities, see e.g. [58–60]. A tiny fraction of SiC grains is formed from core-collapse supernova material. Consequently, these so-called type X and C grains are particularly interesting, since a detailed picture of the interior structure of the progenitor from their abundance distributions can be derived [61,62].

Recently, peculiar isotopic signatures were found in several type C SiC grains in striking disagreement with any existing model [63–65]. They are formed during a core-collapse supernova and are most probably produced at the bottom of the so-called C/Si zone. Some grains show high enrichments in heavy silicon together with light sulfur (^{32}S). These isotopic ratios can not be explained by means of any stellar process, like *ad-hoc* mixing or molecule chemistry. As such, the occurrence of highly enriched ^{32}S constitutes an open question and is so far not resolved.

A possible solution for this problem might come from nuclear physics; neutron captures onto abundant ^{28}Si lead to ^{32}Si , which is a long-

lived radioisotope. With a half-life of roughly 150 years, ^{32}Si is transformed *via* two β^- -decays to stable ^{32}S . To achieve sufficient neutron captures along the Si isotopic chain, enough neutrons need to be produced *in situ*. Calculations have shown that the required neutron densities are in the typical range of the so-called n-process in the core-collapse supernova [66–68]. Combined with the overabundant ^{28}Si at the bottom of the C/Si zone, this explanation of neutron captures leading to ^{32}Si and then decaying into ^{32}S appears to be quite robust. Once the details are well understood, this observation will help constrain stellar parameters during the type II supernovae, like neutron density and wind velocity, among others. This makes this case extremely interesting and valuable for supernova research.

However, some of the required neutron capture cross-sections are not well studied and need experimental validation. Especially, as have been shown in [67], the $^{32}\text{Si}(n,\gamma)$ reaction is uncertain by a factor of 100. This constitutes a serious problem: a $^{28}\text{Si}/^{32}\text{Si}$ ratio is observed in type C SiC grains, but, however, some of the ^{32}Si could be pollution picked up before the grain was implanted into the primitive meteorite roughly a year after the production.

Sensitivity Study

In the sensitivity study presented here, the influence of uncertainties in $^{31}\text{Si}(n,\gamma)^{32}\text{Si}$, $^{32}\text{Si}(n,\gamma)^{33}\text{Si}$ as well as the impact of different neutron densities on the final $^{32}\text{Si}/^{28}\text{Si}$ ratio was studied. This resembles the situation *at situ*; i.e., no transport of the grain through different layers is simulated.

In FIG. 5(top), a part of the nuclear reaction network used is shown. The full nuclear network extends up to ^{56}Mn and consists of neutron capture reactions (n, γ) and corresponding β^- -decays. The network equations are solved using the program NETZ [69].

FIG. 5(bottom) shows the Maxwellian-averaged cross-sections used for $^{31}\text{Si}(n,\gamma)$ and $^{32}\text{Si}(n,\gamma)$ [70,71]. Obviously, the neutron capture rate of $^{31}\text{Si}(n,\gamma)$ is much faster than the subsequent one on ^{32}Si . This is combined with the much shorter half-life of ^{31}Si ($t_{1/2} = 157$ minutes) compared to ^{32}Si ($t_{1/2} = 150$ years). In total, this will lead to a much higher sensitivity of the $^{32}\text{Si}/^{28}\text{Si}$ ratio to uncertainties in the

$^{31}\text{Si}(n,\gamma)$ reaction rate than that induced by the $^{32}\text{Si}(n,\gamma)$ rate.

In a first step, an adequate integrated neutron flux needs to be defined. In FIG. 6, the effect of several integrated neutron fluxes (measured in 1/mb) on the final amount of ^{32}Si is studied. Observationally, a ratio of $^{32}\text{Si}/^{28}\text{Si} \sim 10^{-3}$ has been extracted from the type C SiC grains. To adapt to realistic conditions throughout this study, integrated neutron fluxes should not

exceed 1/mb. In the next step, several different neutron pulse profiles are tested within this approach covering different integrated neutron fluxes in the range given by the vertical lines in FIG. 6. Three typical pulses are shown in FIG. 7. They cover a time-integrated neutron flux from $(10^{-3}$ to $10^{-1})$ 1/mb, which is expected in these scenarios by triggering the efficient $^{22}\text{Ne}(\alpha,n)$ neutron source [67].

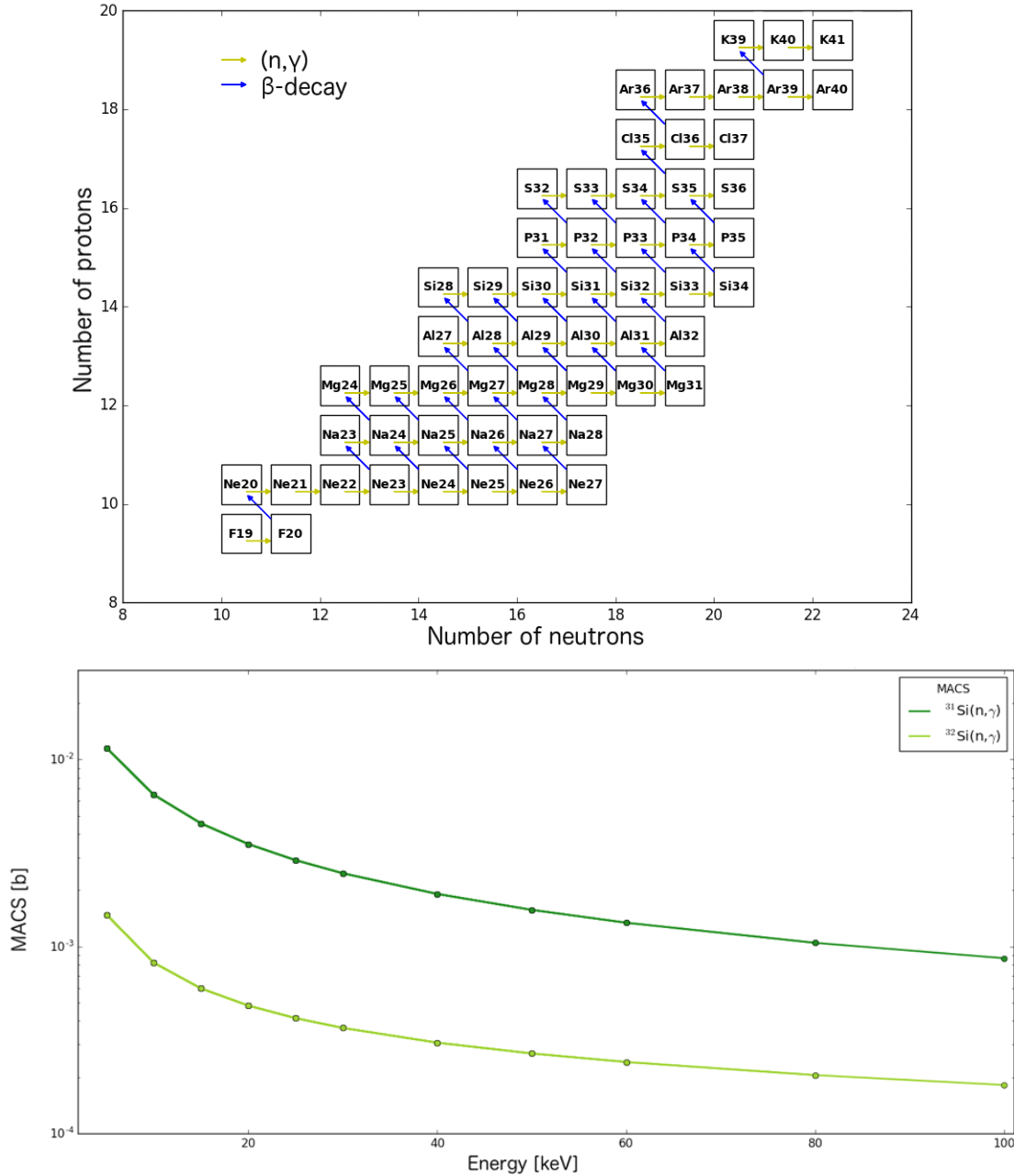


FIG. 5. Part of the network used in this study (top panel). It consists of stable isotopes among a few unstable isotopes. This allows to reconstruct the exact flow path under certain neutron fluxes. The lower panel shows the Maxwellian-averaged cross-sections for $^{31}\text{Si}(n,\gamma)$ and $^{32}\text{Si}(n,\gamma)$ used in this study.

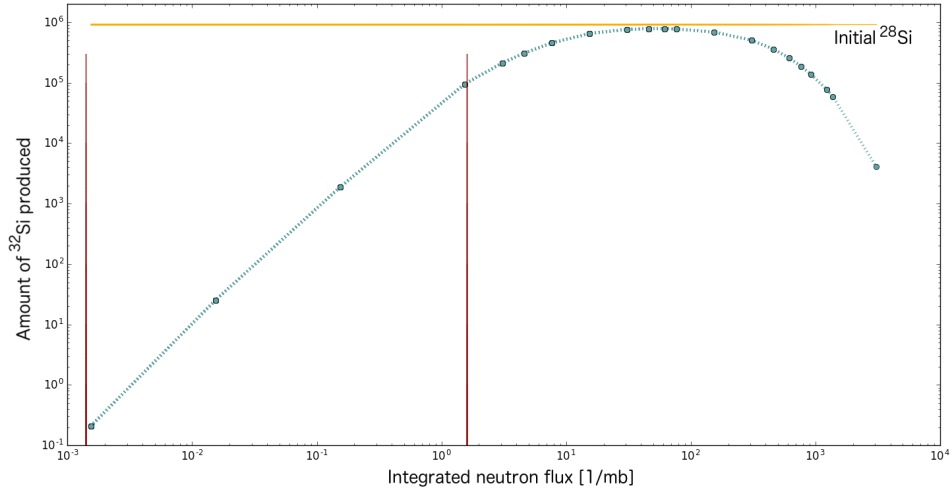


FIG. 6. The effect of different integrated neutron fluxes on the final amount of produced ^{32}Si . The initial amount of ^{28}Si used in this network is shown as a horizontal line. As can clearly be seen, at total neutron fluxes exceeding 1/mb, almost all initial ^{28}Si is transformed into ^{32}Si , which is unrealistic and can be excluded. At integrated neutron fluxes larger than 100/mb, even heavier Si isotopes are produced (^{33}Si and ^{34}Si).

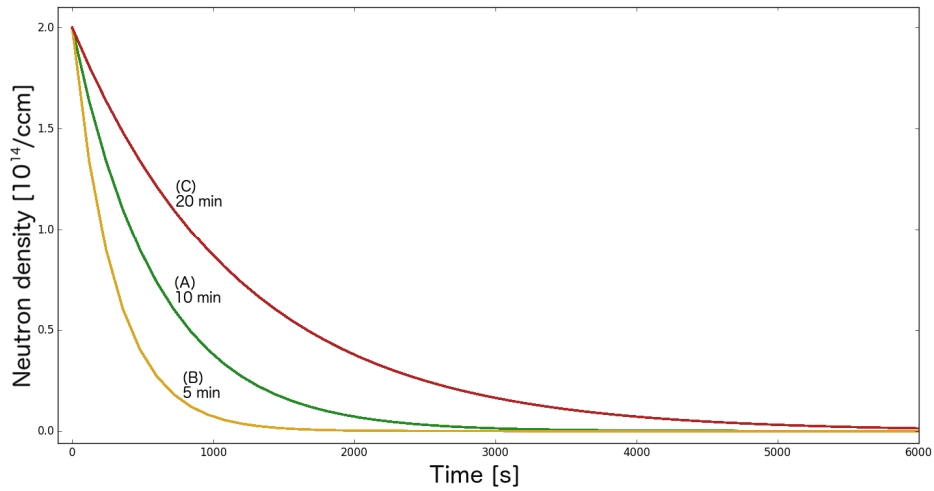


FIG. 7. Three neutron density pulses with a certain characteristic decay time shown next to the lines. Each of the pulses shown here covers a different range of reasonable integrated neutron fluxes.

To assess the effects imposed by uncertainties in the $^{31}\text{Si}(n,\gamma)$ and $^{32}\text{Si}(n,\gamma)$ reaction rate on the final $^{32}\text{Si}/^{28}\text{Si}$ ratio, the rates were varied by a factor of 100 up and down. Moreover, all three neutron pulses A, B and C were used and studied independently.

Here, only the results from pulse A with a decay time of 10 minutes will be presented. However, all other pulses deliver similar results [72]. As can be seen in FIG. 8, the effect of variations in the $^{31}\text{Si}(n,\gamma)$ rate on the $^{32}\text{Si}/^{28}\text{Si}$ ratio is huge. It is obvious that the current uncertainty in the $^{31}\text{Si}(n,\gamma)$ rate is too large to constrain the integrated neutron flux during the type II supernovae explosion.

The situation seems different in the case of variations of $^{32}\text{Si}(n,\gamma)$, as shown in FIG. 9. Here, the observed effect on the $^{32}\text{Si}/^{28}\text{Si}$ ratio appears to be rather small, even negligible at small integrated neutron fluxes. As such, $^{32}\text{Si}(n,\gamma)$ acts as a bottleneck reaction. It is already slow at the relevant temperatures; an even slower rate does not have any impact on the $^{32}\text{Si}/^{28}\text{Si}$ ratio, as shown in FIG. 9. The situation is different when increasing the $^{32}\text{Si}(n,\gamma)$ rate by a certain factor. In FIG. 9, it is obvious that variations of a factor of 100 lead to a small change in the $^{32}\text{Si}/^{28}\text{Si}$ ratio at certain higher integrated neutron fluxes, which is by far not comparable to the changes induced by variations of $^{31}\text{Si}(n,\gamma)$.

This study clearly shows the importance of detailed network calculations. It is evident that the dependence on the $^{31}\text{Si}(n,\gamma)$ reaction rate is much more severe than the sensitivity to changes in the $^{32}\text{Si}(n,\gamma)$ rate. However, constraining the $^{31}\text{Si}(n,\gamma)$ reaction rate is currently only possible using indirect measurements, since the half-life is too short to perform direct (n,γ) experiments. To gain access to this reaction, only indirect techniques, like transfer reactions, Coulomb dissociation [73,74] or others, are applicable.

A typical approach for this problem is to constrain the neighboring reaction rates, like

$^{30}\text{Si}(n,\gamma)$ and $^{32}\text{Si}(n,\gamma)$. Since ^{30}Si is stable, it is possible to produce a target and perform a direct (n,γ) measurement. ^{32}Si is a radioisotope with a long half-life of roughly 150 years. Since the $^{32}\text{Si}(n,\gamma)$ cross-section is rather small at stellar energies, a relatively strong experimental neutron source is required. So far, the existing neutron sources are too weak to perform a direct measurement.

Once the neighboring reactions are constrained experimentally, it is possible to calibrate the reaction theory accordingly and to predict the $^{31}\text{Si}(n,\gamma)$ rate with higher accuracy.

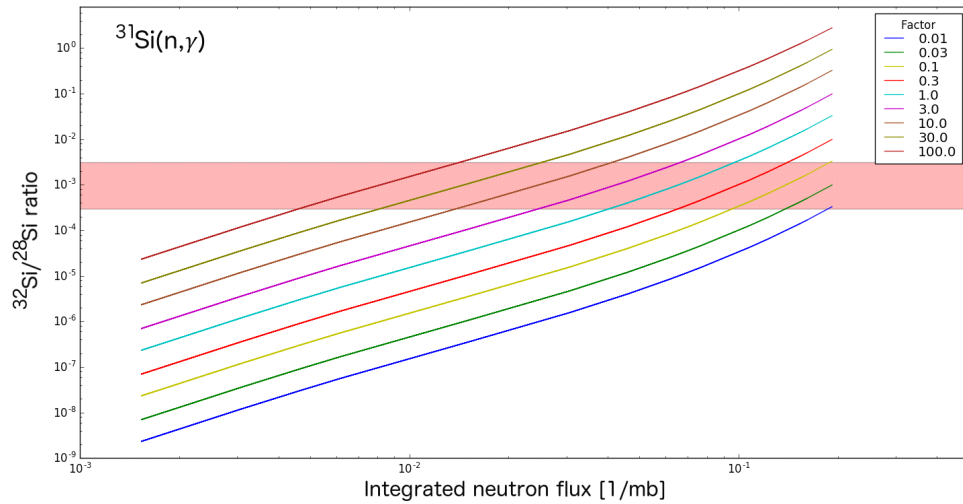


FIG. 8. The $^{31}\text{Si}(n,\gamma)$ reaction rate varied by different factors. All other reaction rates are kept at their nominal value. A dramatic effect on the produced $^{32}\text{Si}/^{28}\text{Si}$ can be observed depending on the integrated neutron flux and the variation of the $^{31}\text{Si}(n,\gamma)$ reaction rate. The horizontal band shows the measured range in SiC grains.

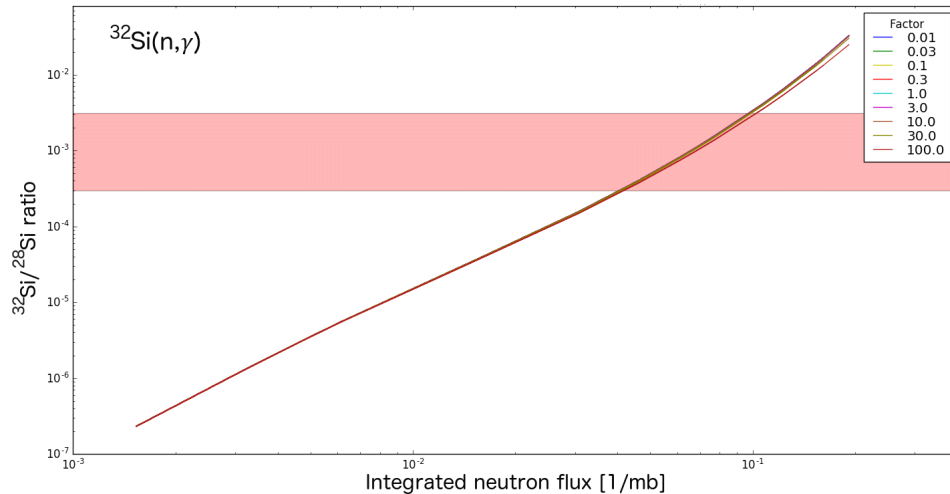


FIG. 9. The effect of variations of $^{32}\text{Si}(n,\gamma)$ on the $^{32}\text{Si}/^{28}\text{Si}$ ratio. It is evident that uncertainties in the rate lead to only minor changes in the produced ^{32}Si abundance over a large range of integrated neutron fluxes. Compared to the changes induced by uncertainties in $^{31}\text{Si}(n,\gamma)$, the effects here are negligible. The horizontal band shows the measured range in the SiC grains.

Conclusion

In this paper, the impact of uncertainties in nuclear reaction rates on two astrophysical processes is examined. In the first case, the rapid proton capture process (rp process) is studied, which powers X-ray bursts on accreting neutron stars. Special emphasis is put on the important ^{56}Ni waiting point nucleus and reaction rate uncertainties of reactions in the vicinity are studied. Already simple network calculations using constant density and temperature can be used to estimate the impact of existing uncertainties and their effect on the observable of these events; X-ray burst light curves. Furthermore, a method is developed for impact studies independent of the detailed temperature and density evolution of single bursts. As shown, $^{59}\text{Cu}(p,\gamma)$ appears to be a very important reaction to be studied in the future.

In the second case, the impact of variations of $^{31}\text{Si}(n,\gamma)$ and $^{32}\text{Si}(n,\gamma)$ is studied regarding the formation of rare SiC type C presolar grains during core-collapse supernovae explosions. It has been shown that variations in $^{31}\text{Si}(n,\gamma)$ have a big effect on the final $^{28}\text{Si}/^{32}\text{Si}$ ratio, which is measured on the SiC grains. Using different example pulses, the detailed effects are investigated and show similar results. The neutron flux, which is created by triggering the $^{22}\text{Ne}(\alpha,n)$ source during the explosion, leads to efficient neutron captures on abundant ^{28}Si towards ^{32}Si , which has a rather long half-life of ~ 150 years and decays after condensation into the SiC grains.

With the advent of upgraded nuclear physics facilities all over the world, these so far inaccessible reaction rates, important for stellar modelling in nuclear astrophysics, can finally be addressed experimentally.

Thereby, it is of utmost importance that these detailed astrophysical and nuclear calculations are used to guide experimental effort. The presented network calculations can be used to reveal important specifics of a certain isotopic region under different temperature and density conditions. Detailed flow extractions and different reasonable thermodynamic trajectories as input parameters are relevant for estimating the impact on the underlying astrophysics in different scenarios and planing future experiments.

At the end, this will lead to efficient usage of already rare and expensive beam time and will help investigate the important open nuclear physics input parameters.

Acknowledgments

The authors thank Hendrik Schatz and Marco Pignatari for valuable discussions. Saed Dababneh acknowledges support from the Alexander von Humboldt Foundation within the Alexander von Humboldt Professorship award. The authors also thank the organizers of the "Jordanian Life Sciences for Sustainable Development" conference for a pleasant experience and fruitful meeting in Jordan.

References

- [1] Rolfs, C.E. and Rodney, W.S., "Cauldrons in the Cosmos: Nuclear Astrophysics", (1988).
- [2] Iliadis, C., "Nuclear Physics of Stars", (2015).
- [3] Burbidge, E.M., Burbidge, G.R., Fowler, W.A. and Hoyle, F., *Rev. Mod. Phys.*, 29 (1957) 547.
- [4] Wallerstein, G., Iben, I., Parker, P., Boesgaard, A. et al., *Rev. Mod. Phys.*, 69 (1997) 995.
- [5] José, J. and Iliadis, C., *Reports Prog. Phys.* 74 (2011) 96901.
- [6] Langer, C., *J. Phys. Conf. Ser.*, 503 (2014) 12022.
- [7] Meisel, Z., *J. Phys. Conf. Ser.*, 742 (2016) 12019.
- [8] Reifarth, R., Lederer, C. and Käppeler, F., *J. Phys. G. Nucl. Part. Physics*, 41(5) (2014) 053101.
- [9] Käppeler, F., Gallino, R., Bisterzo, S. and Aoki, W., *Rev. Mod. Phys.*, 83 (2011) 157.
- [10] Hagen, G., Ekstrom, A., Forssten, C., Jansen, G.R. et al., *Nat. Phys.*, 12 (2016) 186.
- [11] Sherrill, B.M. and Gade, A., *Phys. Scr.*, 91 (2016) 53003.
- [12] Gade, A., Gelbke, C.K. and Glasmacher, T., *Nucl. Phys. News*, 24 (2014) 28.
- [13] Wrede, C., *EPJ Web Conf.*, 93 (2015).

- [14] Spiller, P. and Franchetti, G., Nucl. Instruments Methods Phys. Res. Sect. A, Accel. Spectrometers, Detect. Assoc. Equip. 561 (2006) 305.
- [15] Henning, W., AIP Conf. Proc., 773 (2005) 3.
- [16] Reifarh, R., Altstadt, S., Göbel, K., Heftrich, T. et al., J. Phys. Conf. Ser., 665 (2016) 12044.
- [17] Lewitowicz, M., AIP Conf. Proc., 891 (2007) 91.
- [18] Gales, S., Nucl. Phys. A, 834 (2010) 717c.
- [19] Herlert, A. and Kadi, Y., J. Phys. Conf. Ser., 312 (2011) 52010.
- [20] Lindroos, M., Butler, P.A., Huysse, M. and Riisager, K., Nucl. Instruments Methods Phys. Res. Sect. B Beam Interact. with Mater. Atoms, 266 (2008) 4687.
- [21] Ball, G.C., Buchmann, L., Davids, B., Kanungo, R., Ruiz, C. and Svensson, C.E., J. Phys. G. Nucl. Part. Phys., 38 (2011) 24003.
- [22] https://science.energy.gov/~media/np/nsac/pdf/2015LRP/2015_LRPNS_091815.pdf, Reaching for the Horizon (2015).
- [23] <http://www.nupec.org/lrp2016/Documents/lrp2017.pdf>, Perspectives for Nuclear Physics (2017).
- [24] Aumann, T., Prog. Part. Nucl. Phys., 59 (2007) 3.
- [25] Herlert, A., EPJ Web Conf., 71 (2014).
- [26] Lestinsky, M., Andrianov, V., Aurand, B., Bagnoud, V. et al., Eur. Phys. J. Spec. Top., 225 (2016) 797.
- [27] Berg, G.P.A., Bardayan, D.W., Blackmon, J.C., Chipps, K.A. et al., Nucl. Instruments Methods Phys. Res. Sect. B, Beam Interact. with Mater. Atoms, 376 (2015) 165.
- [28] Baumann, T., Nucl. Instruments Methods Phys. Res. Sect. B, Beam Interact. with Mater. Atoms, 376 (2016) 162.
- [29] Weisshaar, D., Bazin, D., Bender, P.C., Campbell, C.M. et al., Nucl. Instruments Methods Phys. Res. Sect. A, Accel. Spectrometers, Detect. Assoc. Equip., 847 (2017) 187.
- [30] Paschalis, S., Lee, I.Y., MacChiavelli, A.O., Campbell, C.M. et al., Nucl. Instruments Methods Phys. Res. Sect. A, Accel. Spectrometers, Detect. Assoc. Equip., 709 (2013) 44.
- [31] Akkoyun, S., Algora, A., Alikhani, B., Ameil, F. et al., Nucl. Instruments Methods Phys. Res. Sect. A, Accel. Spectrometers, Detect. Assoc. Equip., 668 (2012) 26.
- [32] Langer, C., Montes, F., Aprahamian, A., Bardayan, D.W. et al., Phys. Rev. Lett., 113 (2014) 32502.
- [33] Langer, C., Montes, F., Aprahamian, A., Bardayan, D.W. et al., Inpc 2013, 66 (2013) 1000.
- [34] Ong, W.-J., Langer, C., Montes, F., Aprahamian, A. et al., Phys. Rev. C, 95 (2017) 55806.
- [35] Kankainen, A., Woods, P.J., Nunes, F., Langer, C. et al., Eur. Phys. J. A, 52 (2016) 6.
- [36] Kankainen, A., Woods, P.J., Schatz, H., Poxon-Pearson, T. et al., Phys. Lett. Sect. B, Nucl. Elem. Part. High-Energy Phys., 769 (2016) 549.
- [37] Schatz, H., Aprahamian, A., Barnard, V., Bildsten, L. et al., Phys. Rev. Lett., 86 (2001) 3471.
- [38] Schatz, H., Aprahamian, A., Görres, J., Wiescher, M. et al., Phys. Rep., 294 (1998) 167.
- [39] Fisker, J.L., Brown, E., Liebendoerfer, M., Schatz, H. et al., Astrophysics, 16783 (2004) 4.
- [40] Keek, L., Wolf, Z. and Ballantyne, D.R., Astrophys. J., 826 (2016) 79.
- [41] Cyburt, R.H., Amthor, A.M., Heger, A., Johnson, E. et al., Astrophys. J., 830 (2016) 55.
- [42] Smith, K., Amthor, A.M., Cyburt, R., Ferguson, R. et al., in: Proc. Sci. (2008).
- [43] Parikh, A., José, J., Moreno, F. and Iliadis, C., Astrophys. J. Suppl. Ser., 178 (2008) 110.
- [44] Schatz, H. and Ong, W.J., Astrophys. J., 844 (2017) 139.
- [45] Rehm, K.E. et al., Phys. Rev. Lett., 80 (1998) 676.
- [46] <http://eagle.phys.utk.edu/xnet/trac/> (2017).

- [47] Cyburt, R.H, Amthor, A.M., Ferguson, R., Meisel, Z. et al., *Astrophys. J. Suppl. Ser.*, 189 (2010) 240.
- [48] Köppchen, C., Bachelor thesis, University of Frankfurt, (2016).
- [49] Fryer, C.L., Belczynski, K., Wiktorowicz, G., Dominik, M. et al., *Astrophys. Journal*, 749(1) (2012) 14.
- [50] Fryer, C.L. and Warren, M.S., *Astrophys. Journal*, 574 (2002) L65.
- [51] Janka, H.-T., *Annu. Rev. Nucl. Part. Sci.*, 62 (2012) 407.
- [52] Hansen, C.J., Montes, F. and Arcones, A., *Astrophys. J.*, 797 (2014) 123.
- [53] Travaglio, C., Gallino, R., Amari, S., Zinner, E. et al., *Astrophys. J.*, 510 (1999) 325.
- [54] Hoppe, P. and Zinner, E., *J. Geophys. Res. Sp. Phys.*, 105 (2000) 10371.
- [55] Zinner, E., in: "Treatise Geochemistry" Second Ed. (2013), pp. 181–213.
- [56] Zinner, E., Nittler, L.R., Gallino, R., Karakas, A.I. et al., *Astrophys. J.*, 650 (2006) 350.
- [57] Lodders, K. and Amari, S., *Chemie Der Erde - Geochemistry*, 65 (2005) 93.
- [58] Nittler, L.R., Amari, S., Zinner, E., Woosley, S.E. et al., *Astrophys. J. Lett.*, 462 (1996) L31.
- [59] Hoppe, P., Strebler, R., Eberhardt, P., Amari, S. et al., *Science*, 272 (1996) 1314.
- [60] Amari, S., Nittler, L.R., Zinner, E., Lodders, K. et al., *Astrophys. J.*, 559 (2001) 463.
- [61] Fujiya, W., Hoppe, P., Zinner, E., Pignatari, M. et al., *Astrophys. J.*, 776 (2013) L29.
- [62] Pignatari, M., Wiescher, M., Timmes, F.X., de Boer, R.J. et al., *Astrophys. J. Lett.*, 767 (2013) L22.
- [63] Amari, S., Zinner, E. and Lewis, R.S., *Astrophys. J. Lett.*, 517 (1999) L59.
- [64] Gyngard F., Nittler, L. and Zinner, E., *Meteorit. Planet.*, (2010).
- [65] Xu, Y.C., Amari, S., Gyngard, F., Zinner, E. et al., *Aust. Publ. Meteorit. Planet. Sci. Suppl.*, 75 (2012) 5104.
- [66] Hoppe, P., Fujiya, W. and Zinner, E., *Astrophys. J.*, 745 (2012) L26.
- [67] Pignatari, M., Zinner, E., Bertolli, M.G., Trappitsch, R. et al., *Astrophys. J.*, 771 (2013) L7.
- [68] Meyer, B.S. and Clayton, D.D., *Astrophys. J. Lett.*, 540 (2000) L49.
- [69] [Http://exp-Astro.physik.uni-Frankfurt.de/netz/](http://exp-Astro.physik.uni-Frankfurt.de/netz/) (2017).
- [70] Dillmann, I., Heil, M., Käppeler, F., Plag, R. et al., in: *AIP Conf. Proc.* (2006), p.123.
- [71] Dillmann, I., Plag, R., Käppeler, F., Mengoni, A. et al., in: *Proc. Sci.*, (2014).
- [72] Klapper, N., Bachelor thesis, University of Frankfurt, (2016).
- [73] Langer, C., Lepyoshkina, O., Aksyutina, Y., Aumann, T. et al., *Phys. Rev. C*, 89 (2014) 35806.
- [74] Marganiec, J., Novo, S.B., Typel, S., Langer, C. et al., *Phys. Rev. C*, 93 (2016) 45811.